Journal of Cleaner Production 292 (2021) 126022

Contents lists available at ScienceDirect

Journal of Cleaner Production

journal homepage: www.elsevier.com/locate/jclepro

New superstructure-based model for the globally optimal synthesis of refinery hydrogen networks

Chenglin Chang [a], Zuwei Liao [b, *], Miguel J. Bagajewicz [c, d]

[a] Zhejiang Provincial Key Laboratory of Advanced Chemical Engineering Manufacture Technology, College of Chemical and Biological Engineering, Zhejiang University, Hangzhou, 310027, PR China
[b] State Key Laboratory of Chemical Engineering, College of Chemical and Biological Engineering, Zhejiang University, Hangzhou, 310027, PR China
[c] School of Chemical, Biological and Materials Engineering, University of Oklahoma, Norman, OK, USA
[d] Federal University of Rio de Janeiro (UFRJ), Escola de Química CT, Bloco E, Ilha Do Fundão, CEP 21949-900, Rio de Janeiro, RJ, Brazil

ARTICLE INFO

Article history:
Received 6 October 2020
Received in revised form
2 January 2021
Accepted 15 January 2021
Available online 20 January 2021

Handling editor. Kathleen Aviso

Keywords:
Hydrogen networks synthesis
New superstructure
Mixed integer nonlinear model
Global optimality

ABSTRACT

This work presents a new superstructure for refinery hydrogen networks synthesis. The superstructure eliminates the need to have the pressures of compressors as variables, while both dedicated and shared compressors can be included. As a result of considering the pressures as the parameters known a-priori, the constraint of compression power is expressed by using linear equation. Hydrogen networks synthesis is then formulated as a new mixed integer nonlinear model whose nonlinearities are only attributed to the bilinear and concave terms. The proposed model is a simple optimization problem that could be solved to global optimality. Four literature examples and an industrial case are tested for illustration purpose. The obtained solution results exhibit 3.1−4.5 % reduction in the total annualized cost compared with those of literature ones.

1. Introduction

Hydrogen is a renewable energy and resource widely used in petroleum refineries. Especially due to the limited crude oil supply and the stricter environmental legislations, more and more hydrogen gases are consumed to produce light fuel (Elsherif et al., 2015), electricity (Rezaie et al., 2020) and other commodities (Deng et al., 2019) for sustainable developments in recent decades. The internal hydrogen sources of refinery, such as continuous and semi-regenerative catalytic reformers as well as the gas processing units, are commonly not capable of providing enough fresh hydrogen gases to meet the requirement of hydrogen consumers (Lou et al., 2019; Zhang et al., 2020), such as hydro-treaters, hydro-crackers, olefin saturation, lubricant and isomerization units. Consequentially, most of refineries depend on onsite generations and merchant sources which provide approximately pure hydrogen gases at high prices (Fonseca et al., 2008). Such a serious challenge highlights the importance of refinery hydrogen networks (HN) design wherein hydrogen could be reused among hydrogen source and sink units, significantly saving fresh hydrogen and expenses.

The two most popular approaches to optimal HN design are Pinch Technology (PT) and mathematical modeling by using mathematical programming (MP), although a few attempts to use metaheuristics/stochastic-based methods exist. The former is an insight-based tool inspired by heat integration works (Čuček et al., 2019; Chang et al., 2020) and extended to HN design researches (Bandyopadhyay et al., 2019; Huang and Liu, 2019). For example, Towler et al. (1996) pioneered PT to investigate hydrogen gas distribution using value composite curve. Their analysis exhibited PT provided clear insights to the economic tradeoff for refinery hydrogen management. However, they didn't handle the physically operational constraints which strongly affected HN designs. Considering this, Alves and Towler (2002) captured the operation constraints by cautiously extracting the input data of the sources and sinks. They utilized hydrogen surplus diagram to estimate the minimum fresh hydrogen supplied to networks. In addition, several practical issues such as purifications (Shehata and Shoaib., 2015; Li et al., 2019), multiple components (Umana et al., 2014; Wei et al., 2017) and flowrate fluctuations (Wei et al., 2019) were studied using PT. However, PT is essentially a graphical tool not capable of

* Corresponding author.
E-mail address: liaozw@zju.edu.cn (Z. Liao).

https://doi.org/10.1016/j.jclepro.2021.126022
0959-6526/

optimizing operation and capital expenses simultaneously (Hong et al., 2019; Ebrahimi et al., 2020).

On the other hand, MP method sets up an equation-based mixed integer nonlinear model (MINLM) based on process superstructure. Such an MINLM solved using mixed integer nonlinear programming (MINLP) procedures can handle the problems in a more rigorous manner, allowing the introduction of structural and operational details that PT cannot accommodate (Li et al., 2020). A seminal attempt to HN design optimization by using MP method was initiated by Hallale and Liu (2001). They built a comprehensive superstructure to encompass all possible connections for retrofitting an original network. Afterwards, Liu and Zhang (2004) used the superstructure of Hallale and Liu (2001) to select purifiers for HN retrofit design. They established an MINLM and then relaxed it as a mixed integer linear model, whose solutions later provided the initial values to the original MINLM. This useful superstructure was further explored by Kumar et al. (2010) to optimize the flowrate of recycled hydrogen gas. They compared different models and concluded MINLP was the most realistic approach. Furthermore, Elkamel et al. (2011) integrated refineries' planning models into HN design to comply with several industrial scenarios. An MINLM was built to retrofit new compressor and purifier for maximizing the economic profits of refineries. Birjandi et al. (2014) developed a global optimization strategy for HN design. The authors convexified their MINLM through linear relaxation that together with bound contraction procedures (Faria and Bagajewicz, 2012) was used to globally solve retrofit design problems. Jagannath et al. (2018) established a proper superstructure, wherein recycle compressor (RC) is dedicated to each process unit while makeup compressor (MC) might be shared by multiple gas streams. A heuristic method was proposed to manually assign the MCs' pressures as constant values, but the authors emphasized and warned their heuristic method was not rigorous. This is because there are too many assignment possibilities and some of them might be missed heuristically. Liao et al. (2010) proposed a systematic method for HN retrofit design that used a state-space superstructure integrating purifier. All the possible placements of the devices like compressor and purifier were incorporated in their model. Recently, Rezaie et al. (2020) examined hydrogen management using MINLP model whose outcome was retrofitting hydrogen network and determining hydrogen surplus capacity. Different scenarios were proposed and analyzed to effectively utilize surplus hydrogen with an application to an industrial case in Iranian.

The above works using MP methods mostly focused on hydrogen networks retrofit (HNR), which addresses the redesigns of an existing HN already present. Besides HNR, the grass-roots synthesis of hydrogen network is another aspect of HN design, which is namely hydrogen networks synthesis (HNS) in previous research (Marques et al., 2017). Note that HNS beforehand synthesizes networks from scratch knowing only the input data of hydrogen sources and sinks. In HNR problems, however, the capacities of the existing devices in the original networks like compressors and pipelines are known in advance. Especially, the suction and discharge pressures of the existing compressor are typically designed for the specified operation conditions and cannot be changed during optimization. For instance, Jagannath et al. (2014) researched HNS using an improved superstructure, wherein the conditioning devices like heaters, coolers and valves were embedded. The key feature of their superstructure was the arrangement of the dedicated compressor on each gas transfer line, as depicted in Fig. 1a. In their optimized networks, however, many dedicated compressors were installed, resulting in high capital expenses. To counter this, Jagannath and Almansoori (2017) developed a superstructure in which MC was shared by multiple streams, as shown in Fig. 1b. The RCs in the superstructure were still dedicated to process units complying with industry practices. They modelled an MINLM for HNS to optimize compression costs with the minimum fresh hydrogen supplies. Kang et al. (2019) had investigated the impacts of HNS schemes on networks' flexibilities and economy according to the connection patterns among hydrogen sources and sinks. Direct, indirect and hybrid schemes were researched involving multi-period operations. However, their MP model was computationally ineffective since it rendered numerous local solutions.

Thus far, it should be noted that the MCs in the above discussed superstructures are allocated either in the dedicated form (Fig. 1a) or the shared form (Fig. 1b). In the former one, there is an available MC dedicated on every transfer line (Deng et al., 2020). The suction (discharge) pressure is the pressure of the source (sink) that sends (receives) gas to (from) MC. Thus, the compression power is calculated by a linear equation since the pressures of MCs are known beforehand. Nevertheless, as in this option, MC cannot be shared by multiple gas streams and there exists a waste of equipment resources. This may result in many dedicated compressors present in the optimized network, increasing capital investment. In the latter one (Fig. 1b), shared MCs are allocated among multiple streams, which was an efficient usage of equipment resource (Jhaveri et al., 2014). The total number of compressors and capital expenses are thereby decreased, as illustrated by Jagannath and Almansoori (2017). Nevertheless, they defined the suction (discharge) pressure of MC as a variable. Consequentially, the compression power equation in their MINLM involved highly nonlinear constraint making HNS into a computationally-hard model. Hence, the authors employed a time limit (4 h) when solving case studies, showing their MINLM had convergence problems. From these above, one can find the model using dedicated form (Fig. 1a) is easy to solve but suffers from limited structure possibilities while the model using shared form (Fig. 1b) is rich in structure possibilities but difficult to solve. There lacks a mathematical model which can balance the richness of structure possibilities and the computational difficulties, while this is the goal of the present work.

To derive such a mathematical model, a new superstructure is developed for HNS in this study. In this superstructure, there exists an available compressor (dedicated one) on each gas transfer line whose inlet and outlet pressures are known beforehand. Hence, the compressors with different pressure combinations are included in the superstructure. Besides dedicated compressors, the shared compressors are also involved by assigning compressor after a set of mixer-splitter nodes whose pressures are specified as the outlet pressures of all hydrogen sources. The compression power is therefore expressed using linear equation. The resulting MINLM could automatically make choices among these compressors and only the gas flowrates of compressors demand to be determined. The nonlinearities of this MINLM are only attributed to the bilinear terms in concentration (purity) balances and concave terms for the equipment costs. This paper is constructed as follows. Section 2 states the generic definition for HNS problem with the established superstructure. Section 3 presents all constraints and objective function of the MINLM. Examples are solved in Section 4 and conclusion is summarized finally.

2. Problem statement and superstructure

The problem of HNS in refineries can be generally stated as follows. Given several hydrogen-producing units ($i \in IS$) namely hydrogen utility sources which provide fresh hydrogen with constant purity (Y_i), outlet pressure (P_i) and flowrate bounds ($Fmin_i$ and $Fmax_i$). Given also several hydrogen-consuming units ($u \in US$),

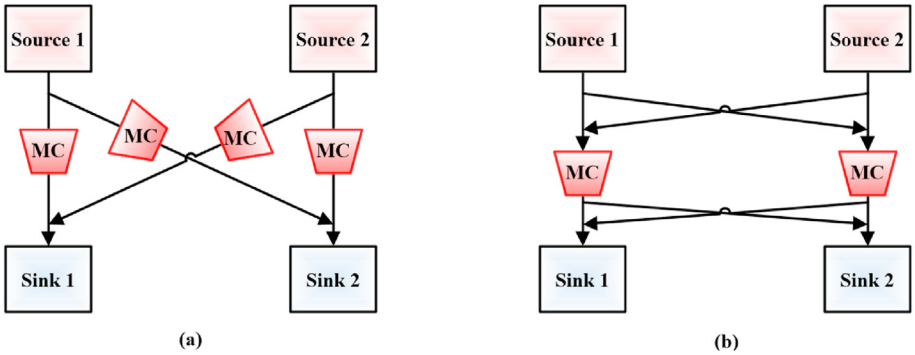

Fig. 1. Allocation of available compressors: (a) dedicated compressors; (b) shared compressors.

namely process units feeding hydrogen gas with fixed flowrate (F_u^{in}), pressure (P_u^{in}) and limited purity (Y_u^{in}). After consuming some pure hydrogen, each process unit gives out off-gas with the fixed flowrate (F_u^{out}), pressure (P_u^{out}) and purity (Y_u^{out}). The off-gases can be reused between process units, or directed to purifiers ($t \in TS$) for hydrogen purification, or disposed to fuel gas sinks ($j \in JS$) after the desulphurization. Here, each purifier is characterized by fixed inlet pressure (P_t), hydrogen recovery ratio (R_t), a product stream with fixed pressure (P_t^{pro}) and purity (Y_t^{pro}), and a residue stream with fixed pressure (P_t^{res}). The objective is to synthesis a network with minimum total annualized cost (TAC) including capital investments and operational expenses. To simplify the problem under study, the following assumptions are made.

1. All the gas streams in network are the mixtures of only hydrogen and methane. The other components in much smaller proportion, such as ethane, propane, etc., are all ignored and lumped with methane. The key component of gas is hydrogen (purity).
2. Because hydrogen has a behavior very close to ideal, the ideal gas law is used.
3. The given input data of all hydrogen origin and destination units, such as hydrogen utility sources, process units, purifiers and fuel gas sinks (FGS) are constants.
4. Each compression process is single-stage and adiabatic with the fixed index (γ) and efficiency (η), while compressors could be allocated in series.
5. The suction temperature ($\widehat{T}$) of compressor is 298.15 K (25.0 °C) and the demanded heating and/or cooling costs are neglected.
6. The pressure drops are zero in pipelines and no phase change occurs in networks.
7. The manufacturer's limitations of all devices' capacities are given prior to HNS.

In this research, a set of mixer-splitter nodes ($m \in MS$) are added into hydrogen network for establishing the superstructure in Fig. 2. The pressures (P_m) of these mixer-splitter nodes ($MS = \{IS \cup US \cup TS\}$) are specified as the pressures of hydrogen origin units, such as utility sources (P_i), process units (P_u^{out}) and purifiers (P_t^{pro} and P_t^{res}). In Fig. 2, there are in total seven blocks of units, respectively being utility sources, outlet of process units, outlet of purifiers, mixer-splitter nodes, FGS, inlet of process units and inlet of purifiers. These blocks are all modelled with mixers or/and splitters which are connected to each other. Although the compressors are dedicated on gas transfer line, shared compressor can exist in the finally optimized networks due to the presences of the added mixed-splitter nodes, which is different from the previous researches. For mixer-splitter node m, it only can be connected to the source (sink), whose pressure is lower (larger) than or equal to P_m. The residue gas of purifier is disposed to FGS after desulphurization (Wang et al., 2016), since its purity is relatively low (Jagannath et al., 2014). The index r ($r \in RS$) is used to represent source units ($RS = \{IS \cup US \cup MS \cup TS\}$) and index k ($k \in KS$) to represent sink units ($KS = US \cup MS \cup TS \cup JS$). The schematic diagrams of the above units are depicted in Fig. 3.

3. MINLM formulation

In this section, an MINLM is formulated for HNS based on the superstructure in Fig. 2. This section is divided into four subsections namely material balance, connection constraints, compression constraints, along with cost calculation and objective function. Their detailed formulations are in the following paragraphs. The definitions of the used indices, sets, variables and parameters are listed in Part A of Supplemental Information.

3.1. Material balance

As presented in Fig. 3a, hydrogen utility source i provides fresh hydrogen (f_i) to process units ($f_{i,u}$), mixer-splitter nodes ($f_{i,m}$), purifiers ($f_{i,t}$) and FGS ($f_{i,j}$). Hence, the following mass balance and flowrate limit are demanded for utility source i.

$$f_i = \sum_{u \in US} f_{i,u} + \sum_{\substack{m \in MS \\ P_i \le P_m}} f_{i,m} + \sum_{t \in TS} f_{i,t} + \sum_{j \in JS} f_{i,j} \quad \forall i \in IS \tag{1}$$

$$Fmin_i \le f_i \le Fmax_i \quad \forall i \in IS \tag{2}$$

Fig. 3b shows that process unit u receives fed hydrogen gas from hydrogen utility sources, process units ($f_{u',u}$), mixer-splitter nodes ($f_{m,u}$) and the product of purifiers ($f_{t,u}^{pro}$). Its inlet mass and purity/concentration balances are respectively:

$$F_u^{in} = \sum_{i \in IS} f_{i,u} + \sum_{u' \in US} f_{u',u} + \sum_{\substack{m \in MS \\ P_m \le P_u^{in}}} f_{m,u} + \sum_{t \in TS} f_{t,u}^{pro} \quad \forall u \in US \tag{3}$$

$$F_u^{in} \cdot Y_u^{in} \le \sum_{i \in IS} f_{i,u} \cdot Y_i + \sum_{u' \in US} f_{u',u} \cdot Y_{u'}^{out} + \sum_{\substack{m \in MS \\ P_m \le P_u^{in}}} f_{m,u} \cdot y_m + \sum_{t \in TS} f_{t,u}^{pro} \cdot Y_t^{pro} \quad \forall u \in US \tag{4}$$

Process unit u also directs its off-gas to process units ($f_{u,u'}$),

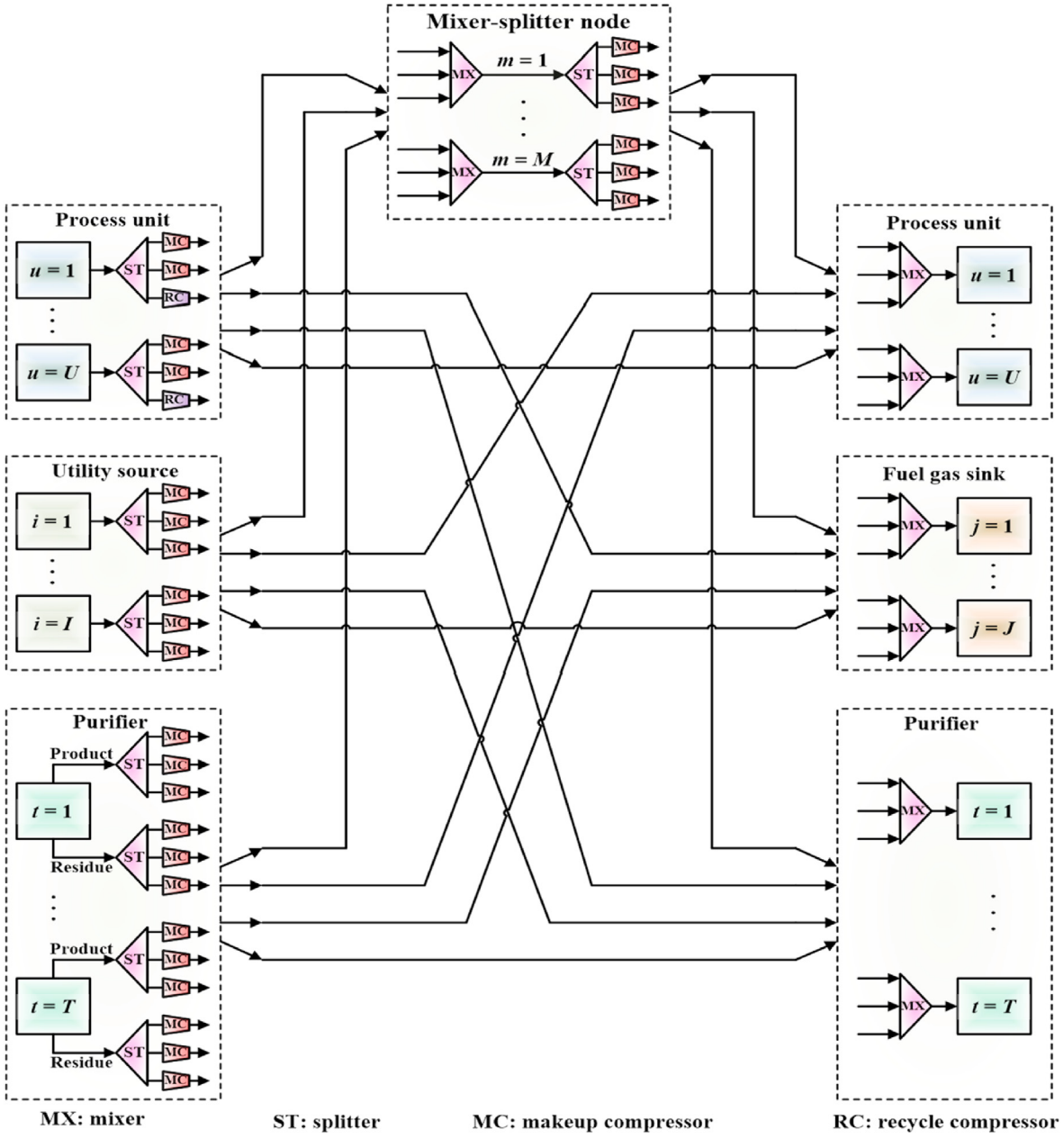

Fig. 2. The proposed superstructure for HNS.

mixer-splitter nodes ($f_{u,m}$), purifiers ($f_{u,t}$) and FGS ($f_{u,j}$), thus its outlet mass balance is:

$$F_u^{out} = \sum_{u' \in US} f_{u,u'} + \sum_{\substack{m \in MS \\ P_u^{out} \le P_m}} f_{u,m} + \sum_{t \in TS} f_{u,t} + \sum_{j \in JS} f_{u,j} \quad \forall u \in US \tag{5}$$

As presented in Fig. 3c, mixer-splitter node m receives gases from hydrogen utility sources, process units and the product of purifiers ($f_{t,m}^{pro}$), hence its inlet mass and purity balances are the following ones:

$$f_m = \sum_{\substack{i \in IS \\ P_i \le P_m}} f_{i,m} + \sum_{\substack{u \in US \\ P_u^{out} \le P_m}} f_{u,m} + \sum_{\substack{t \in TS \\ P_t^{pro} \le P_m}} f_{t,m}^{pro} \quad \forall m \in MS \tag{6}$$

$$f_m \cdot y_m = \sum_{\substack{i \in IS \\ P_i \le P_m}} f_{i,m} \cdot Y_i + \sum_{\substack{u \in US \\ P_u^{out} \le P_m}} f_{u,m} \cdot Y_u^{out} + \sum_{\substack{t \in TS \\ P_t^{pro} \le P_m}} f_{t,m}^{pro} \cdot Y_t^{pro} \quad \forall m \in MS \tag{7}$$

The mixer-splitter node m also send gas to process units, purifiers ($f_{m,t}$) and FGS ($f_{m,j}$), and its outlet mass balance is:

$$f_m = \sum_{\substack{u \in US \\ P_m \le P_u^{in}}} f_{m,u} + \sum_{\substack{t \in TS \\ P_m \le P_t}} f_{m,t} + \sum_{\substack{j \in JS \\ P_m \le P_j}} f_{m,j} \quad \forall m \in MS \tag{8}$$

Fig. 3d depicts purifier t receives gas from hydrogen utility sources, process units, mixer-splitter nodes and other purifiers

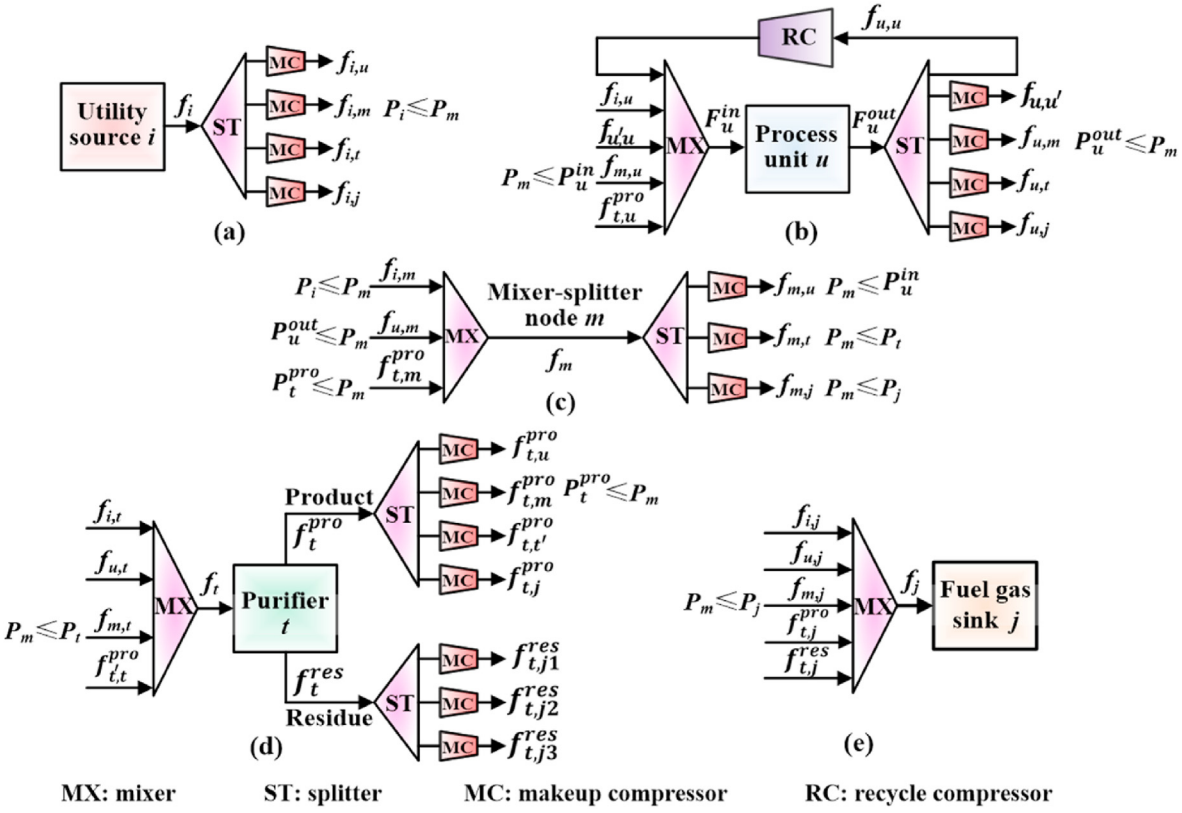

Fig. 3. Schematic diagram of each unit for HNS: (a) utility source; (b) process unit; (c) mixer-splitter node; (d) purifier; (e) fuel gas sink.

($f^{pro}_{t',t}$). Its inlet mass and purity balances are:

$$f_t = \sum_{i\in IS} f_{i,t} + \sum_{u\in US} f_{u,t} + \sum_{\substack{m\in MS \\ P_m \le P^{pro}_t}} f_{m,t} + \sum_{\substack{t'\in TS \\ t'\neq t}} f^{pro}_{t',t} \quad \forall t\in TS \tag{9}$$

$$f_t \cdot y_t = \sum_{i\in IS} f_{i,t}\cdot Y_i + \sum_{u\in US} f_{u,t}\cdot Y^{out}_u + \sum_{\substack{m\in MS \\ P_m \le P^{pro}_t}} f_{m,t}\cdot y_m + \sum_{\substack{t'\in TS \\ t'\neq t}} f^{pro}_{t',t}\cdot Y^{pro}_{t'} \quad \forall t\in TS \tag{10}$$

$$f_t \le z_t \cdot f^{up}_t \quad \forall t\in TS \tag{11}$$

where y_t denotes the purity of the mixed gas to purifier t; z_t denotes the existence of purifier t. After purification, the product (f^{pro}_t) and residue (f^{res}_t) gases are produced out of purifier. Like some contemporary study (Khajehpour et al., 2009), in this research the hydrogen recovery ratio and the product gas purity of each purifier are both constant parameters. Thus, purifier t also has the following outlet mass and purity balances:

$$f_t = f^{pro}_t + f^{res}_t \quad \forall t\in TS \tag{12}$$

$$f^{pro}_t \cdot Y^{pro}_t = R_t \cdot f_t \cdot y_t \quad \forall t\in TS \tag{13}$$

$$f^{res}_t \cdot y^{res}_t = (1-R_t)\cdot f_t \cdot y_t \quad \forall t\in TS \tag{14}$$

where y^{res}_t represents the purity of residue gas leaving purifier t.

The product of purifier t could be sent to process units, mixer-splitter nodes, other purifiers ($f^{pro}_{t,t'}$) and FGS. Hence, the following mass balance is demanded:

$$f^{pro}_t = \sum_{u\in US} f^{pro}_{t,u} + \sum_{\substack{m\in MS \\ P^{pro}_t \le P_m}} f^{pro}_{t,m} + \sum_{\substack{t'\in TS \\ t'\neq t}} f^{pro}_{t,t'} + \sum_{j\in JS} f^{pro}_{t,j} \quad \forall t\in TS \tag{15}$$

The residue gas of purifier t is discharged to FGS after desulphurization, since its purity is relatively low, thus,

$$f^{res}_t = \sum_{j\in JS} f^{res}_{t,j} \quad \forall t\in TS \tag{16}$$

Fig. 3e presents each FGS receives gas (f_j) from hydrogen utility sources, process units, mixer-splitter nodes as well as the product and residue of purifiers. Its mass and purity balances are written as:

$$f_j = \sum_{i\in IS} f_{i,j} + \sum_{u\in US} f_{u,j} + \sum_{\substack{m\in MS \\ P_m \le P_j}} f_{m,j} + \sum_{t\in TS} f^{pro}_{t,j} \quad \forall j\in JS \tag{17}$$

$$f_j \cdot y_j = \sum_{i\in IS} f_{i,j}\cdot Y_i + \sum_{u\in US} f_{u,j}\cdot Y^{out}_u + \sum_{\substack{m\in MS \\ P_m \le P_j}} f_{m,j}\cdot y_m + \sum_{t\in TS} f^{pro}_{t,j}\cdot Y^{pro}_t \quad \forall j\in JS \tag{18}$$

where y_j denotes the purity of the mixed gas to FGS j.

3.2. Connection constraints

The constraints of the connections among hydrogen utility sources, process units, mixer-splitters, purifiers and FGS are written as follows.

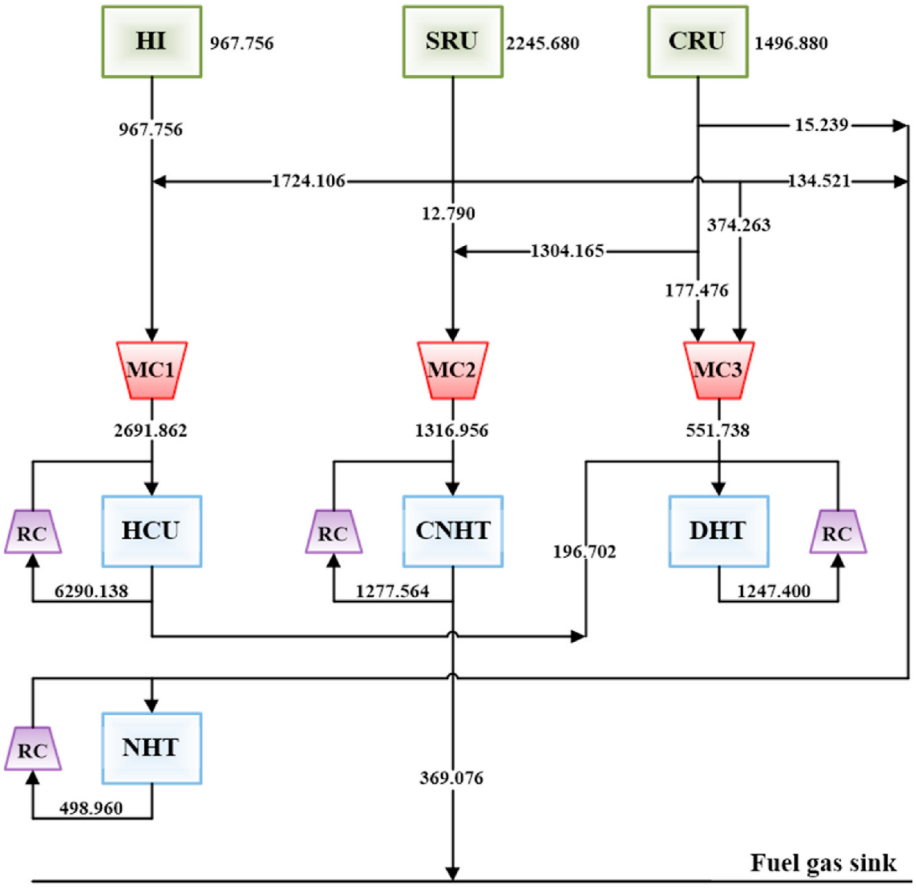

Fig. 4. The optimal network of Jagannath and Almansoori (2017) for example 1.

$$z_{r,k} \cdot f_{r,k}^{lo} \le f_{r,k} \le z_{r,k} \cdot f_{r,k}^{up} \quad \forall r \in RS, k \in KS \tag{19}$$

where $f_{r,k}$ represents the gas flowrate of the connection between each hydrogen source r ($r \in RS$) and hydrogen sink k ($k \in KS$); binary variable $z_{r,k}$ denotes the existence of the connection; $f_{r,k}^{up}$ represents the upper bound of $f_{r,k}$; $f_{r,k}^{lo}$ represents the lower bound of the flowrate if the connection exists. The subscripts r ($r \in RS$) and k ($k \in KS$) are used to respectively represent all the hydrogen sources ($RS = \{IS \cup US \cup MS \cup TS\}$) and sinks ($KS = \{US \cup MS \cup TS \cup JS\}$).

In industrial practice, the recycled hydrogen gases are generally compressed in the recycle compressors only (Liu et al., 2020). For this, the following connection constraint is demanded:

$$z_{u,m} + z_{m,u} \le 1 \quad \forall u \in US, m \in MS \tag{20}$$

3.3. Compression constraints

For each connection, when the pressure of the source (P_r) is lower than that of the sink (P_k), the available compressor on the gas transfer line exists and the compression power is computed by the following polytropic equation:

$$pw_{r,k} = \frac{f_{r,k} \cdot \widehat{R} \cdot \widehat{T}}{3600 \cdot \eta} \cdot \frac{\gamma}{\gamma - 1} \left[\left(\frac{P_k}{P_r} \right)^{\frac{\gamma-1}{\gamma}} - 1 \right] \quad \forall r \in RS, k \in KS \tag{21}$$

where $pw_{r,k}$ represents the power of the compressor between source r and sink k. Eq. (21) is transformed from the one used by Jagannath and Almansoori (2017) based on Ideal Gas State Equation (ideal gas behavior). Note that Eq. (21) is linear constraint since the pressures are both known a-priori.

In this research, the following bounds are given to the compression ratio when the compressor exists:

$$z_{r,k} \cdot Ratio^{min} \le \frac{P_k}{P_r} \quad \forall r \in RS, k \in KS, P_r < P_k \tag{22}$$

$$z_{r,k} \cdot \frac{P_k}{P_r} \le Ratio^{max} \quad \forall r \in RS, k \in KS, P_r < P_k \tag{23}$$

where $Ratio^{min}$ and $Ratio^{max}$ respectively denote the minimum and maximum values of the compression ratio.

3.4. Cost calculation and objective function

There are several considerable cost terms in HNS, for example fresh hydrogen cost ($cost^{hyd}$), profit of FGS ($profit^{fgs}$), electricity cost of compressors ($cost^{ele}$), capital cost of compressors ($cost^{com}$), piping cost ($cost^{pip}$) and purifier cost ($cost^{pur}$). These cost terms are respectively calculated by:

$$cost^{hyd} = \sum_{i \in IS} f_i \cdot CH_i \tag{24}$$

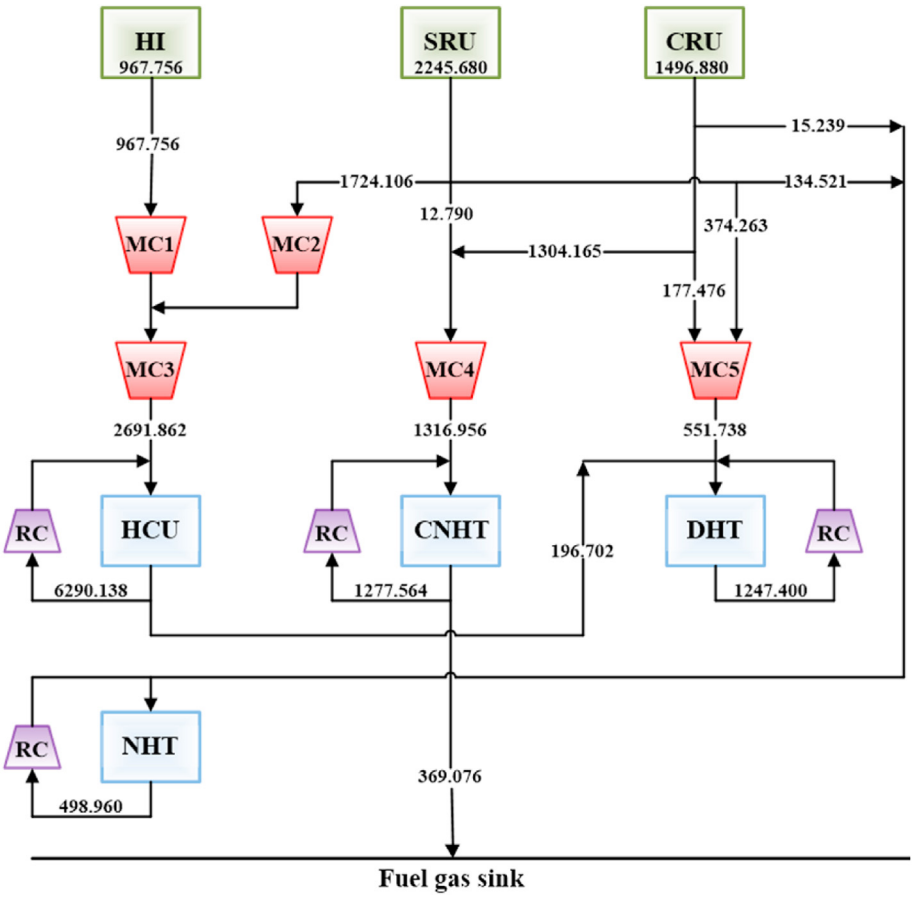

Fig. 5. The network design of the globally optimal solution for example 1.

Table 1
Solution comparison for example 1.

Item	Solution in literature [Ref]	Solution in this work
Hydrogen flowrate (kmol/h)	4710.316	4710.316
Number of compressors	7	9
Compression power (kW)	11,582.5	10,921.9
Electricity cost ($/y)	3,043,882.4	2,870,284.0
Capital cost of compressors ($/y)	589,939.5	651,786.2
Computing time (s)	14,400.0	812.6
TAC ($/y)	3,633,821.9	3,522,070.2

Ref: Jagannath and Almansoori (2017).

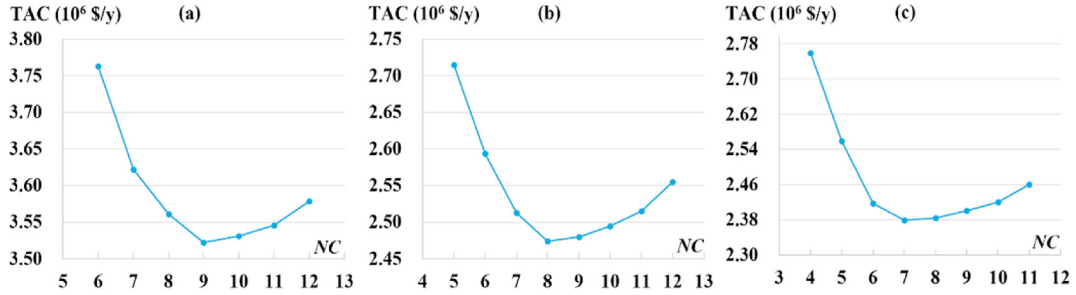

Fig. 6. The sensitivity analysis of the total number of compressors (*NC*): (a) example 1; (b) example 2; (c) example 3.

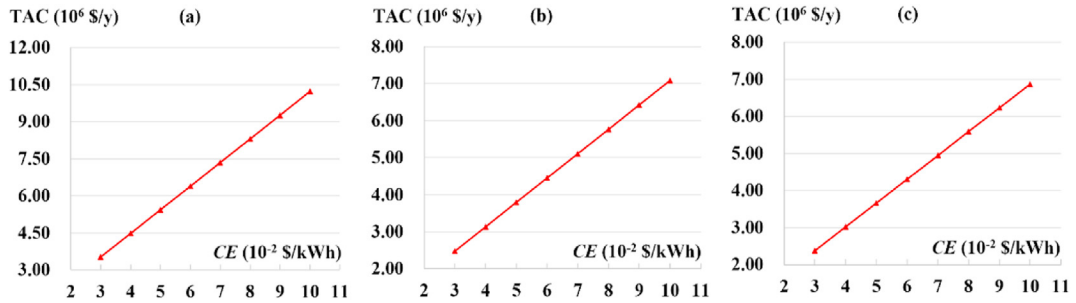

Fig. 7. The sensitivity analysis of electricity price (*CE*): (a) example 1; (b) example 2; (c) example 3.

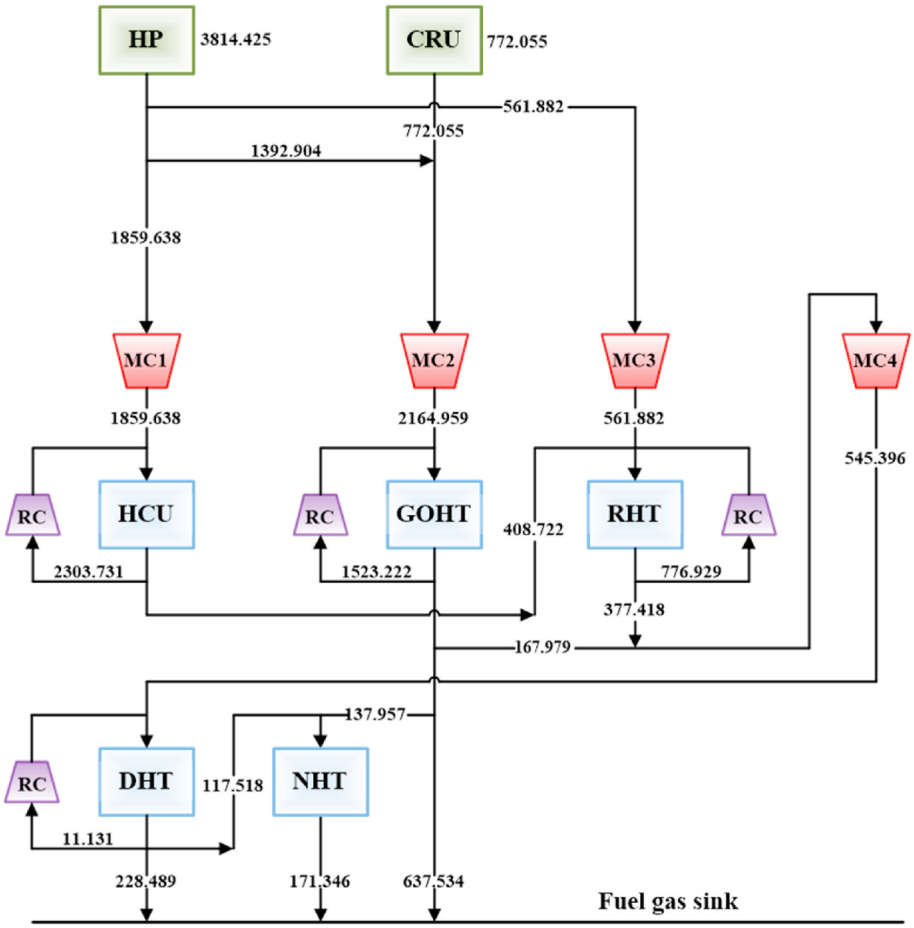

Fig. 8. The optimal network of Jagannath and Almansoori (2017) for example 2.

$$profit^{fgs} = 10^3 \cdot Hour \cdot CF \cdot \sum_{j \in JS} f_j \cdot \left[y_j \cdot HV^{H2} + \left(1 - y_j\right) \cdot HV^{CH4} \right] \tag{25}$$

$$cost^{ele} = Hour \cdot CE \cdot \sum_{r \in RS} \sum_{k \in KS} pw_{r,k} \tag{26}$$

$$cost^{com} = \sum_{r \in RS} \sum_{k \in KS} AF \cdot \left(a \cdot z_{r,k} + b \cdot pw_{r,k}^{c} \right) \tag{27}$$

$$cost^{pip} = AF \cdot \left[\sum_{r \in RS} \sum_{k \in KS} L_{r,k} \cdot \left(\alpha^{pip} \cdot z_{r,k} + \beta^{pip} \cdot f_{r,k} \right) \right] \tag{28}$$

$$cost^{pur} = AF \cdot \sum_{t \in TS} \left(\alpha^{pur} \cdot z_t + \beta^{pur} \cdot f_t \right) \tag{29}$$

where CH_i denotes the price of fresh hydrogen; *Hour* denotes annual operation hours; HV^{H2} and HV^{CH4} are respectively the standard heat of burning hydrogen and methane; *CE* denotes electricity price; *AF* denotes the annualized factor of capital expenses; *a*, *b* and *c* are the cost coefficients of compressors; α^{pip} and β^{pip} are the cost coefficients of pipeline; $L_{r,k}$ denotes the distance between source *r* and sink *k*; α^{pur} and β^{pur} denote the cost

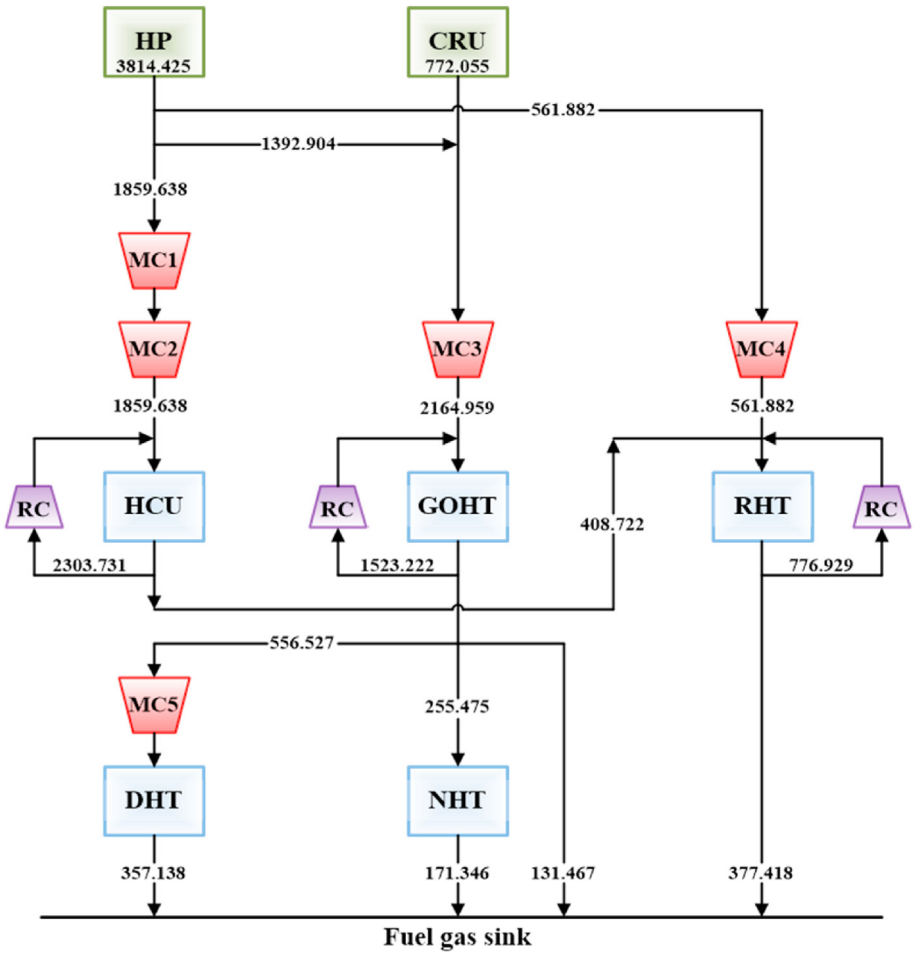

Fig. 9. The network design of the globally optimal solution for example 2.

Table 2
Solution comparison for example 2.

Item	Solution in literature [Ref]	Solution in this work
Hydrogen flowrate (kmol/h)	4586.480	4586.480
Number of compressors	8	8
Compression power (kW)	7974.8	7518.5
Electricity cost ($/y)	2,095,776.9	1,975,848.7
Capital cost of compressors ($/y)	494,204.6	498,142.1
Computing time (s)	14,400.0	936.5
TAC ($/y)	2,589,981.5	2,473,990.8

Ref: Jagannath and Almansoori (2017).

coefficients of purifiers. Note that the capital expenses of pipelines and purifiers are all linearly related to the gas flowrates (Jagannath et al., 2018).

Based on the above, the objective function of HNS is written as:

$$Min\ TAC = cost^{hyd} - profit^{fgs} + cost^{ele} + cost^{com} + cost^{pip} + cost^{pur} \tag{30}$$

The nonlinearities of the MINLM are attributed to the bilinear terms in Eqs. (4), (7), (10), (13), (14), (18) and (25) and the concave term in Eq. (27).

4. Case studies

In this section, five examples are illustrated in which the former three are the ones without purifier while the other two integrate Pressure Swing Adsorption (PSA) unit as the purifier. All parameter values are provided in Part B of Supplemental Information. The distances among hydrogen sources and sinks ($L_{r,k}$) in each example are all 1000.0 m, and the output data of MCs in the final networks are listed in Part C of Supplemental Information. The superstructure-based MINLM is implemented in GAMS (Brooke et al., 2005), in which BARON is selected as the global solver with optimality tolerance being 10^{-6}. All GAMS computations are implemented without any initial value using a personal computer with Intel® Core™ i5-3600U processor that has 3.2 GHz speed and 6 GB memory, running on windows 10 ultimate 64-bit operating system.

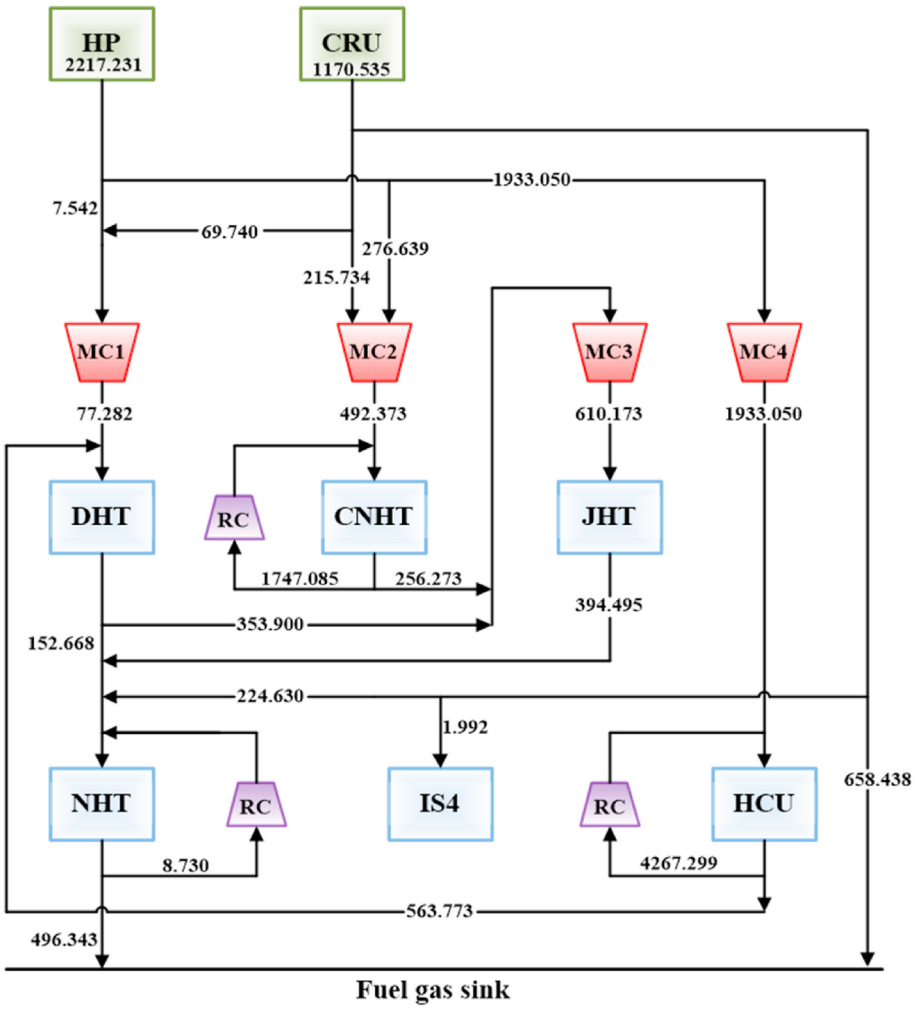

Fig. 10. The optimal network of Jagannath and Almansoori (2017) for example 3.

4.1. Example 1

The first case is adopted from Alves and Towler (2002). It includes three hydrogen utility sources HI, SRU and CRU, four process units HCU, NHT, CNHT and DHT, and one FGS. The sources SRU and CRU provide auxiliary fresh hydrogen gases with fixed flowrates and zero costs. Jagannath and Almansoori (2017) had researched this case to optimize total compression cost under the minimum fresh hydrogen flowrate (4710.316 kmol/h). Only the capital and operational expenses of compressors were included in the TAC, not including fresh hydrogen costs and piping costs. The optimal network of their solution is depicted in Fig. 4 whose TAC is 3,633,821.9 $/y. This figure shows that there are seven compressors demanded, three being makeup ones and four being recycle ones.

To be able to compare results, the total flowrate of fresh hydrogen supply is fixed as the minimum one (4710.316 kmol/h). The proposed superstructure-based model for this example includes 436 constraints, 287 continuous variables and 95 binary variables. After solving in 812.6 s, the globally optimal solution is obtained and its network design is depicted in Fig. 5 with a TAC of 3,522,070.2 $/y. Table 1 lists the cost-related terms of the solutions in literature and this work. This table shows the globally optimal solution requires more compressors (7 vs. 9) which increases capital cost. However, the total compression power demanded is lower (11,582.5 vs. 10,921.9 kW), considerably reducing the electricity expenses. As a result, the TAC is decreased by 3.1% from the solution of Jagannath and Almansoori (2017). Also, the computing time is significantly decreased and the global optimality of the solution can be guaranteed. The sensitivity analysis of the total number of compressors (*NC*) and the electricity price (*CE*) for this example are respectively depicted in Fig. 6a and Fig. 7a. Fig. 6a illustrates that the TAC decreases from $NC = 6$ to 9 and increases from $NC = 9$ to 12. It clearly shows the TAC of the global optimum is sensitive with the total number of compressors. Fig. 7a indicates that TAC is almost linearly related to electricity price and increases monotonically. This illustrates electricity price is a modeling coefficient that has great impact on the globally optimal solutions.

4.2. Example 2

The second case study from Elkamel et al. (2011) consists of two hydrogen utility sources HP and CRU, five process units HCU, GOHT, RHT, DHT and NHT, and one FGS. CRU is an auxiliary source that provides fresh hydrogen gases with fixed flowrate and zero cost. This case study had been studied by Jagannath and Almansoori (2017) to minimize the total compression expenses under the minimum fresh flowrate (4586.480 kmol/h). Thus, to be able make comparison, in this study the flowrate of fresh hydrogen gas is also fixed as the minimum one, ignoring hydrogen and piping costs. The optimal network flowsheet provided by Jagannath and Almansoori

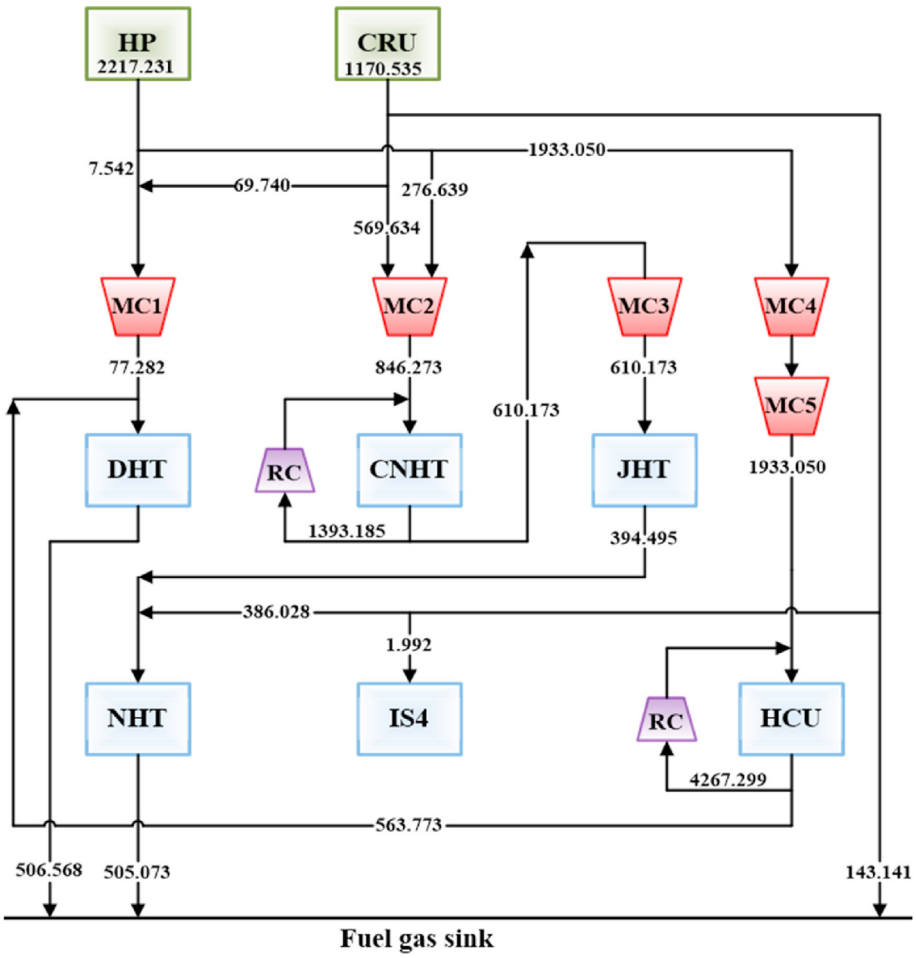

Fig. 11. The network design of the globally optimal solution for example 3.

Table 3
Solution comparison for example 3.

Item	Solution in literature [Ref]	Solution in this work
Hydrogen flowrate (kmol/h)	3387.765	3387.765
Number of compressors	7	7
Compression power (kW)	7742.9	7321.8
Electricity cost ($/y)	2,034,839.1	1,924,169.8
Capital cost of compressors ($/y)	447,253.4	454,565.1
Computing time (s)	14,400.0	1198.6
TAC ($/y)	2,482,092.5	2,378,734.8

Ref: Jagannath and Almansoori (2017).

(2017) is presented in Fig. 8 whose TAC is 2,589,981.5 $/y. This figure shows that there exist eight compressors in total, four being makeup ones and four being recycle ones respectively. Each process unit requires a recycle compressor except NHT whose off-gas is directly sent to FGS.

The superstructure-based MINLM of this case has 589 constraints, 384 continuous variables and 123 binary variables. After running in 936.5 s, the model converges to the global optimum with a TAC of 2,473,990.8 $/y, whose network design is depicted in Fig. 9. For comparison purpose, Table 2 presents the cost breakdowns of the solution obtained in literature and this work. It can be seen from the table that the capital cost of compressor is increased slightly while the electricity expense is considerably decreased. This is because the total compression power is reduced from 7974.8 to 7518.5 kW. The TAC is thereby reduced by 4.5% (2,589,981.5 vs. 2,473,990.8 $/y). More significantly, the global optimality of the solution could be guaranteed while the computing time has been decreased largely, demonstrating the applicability of the proposed superstructure-based MINLM. The sensitivity analysis of the total number of compressors (*NC*) of this example is depicted in Fig. 6b. It illustrates that the TAC decreases from $NC = 5$ to 8 and increases from $NC = 8$ to 12. It can be seen from Fig. 6b that TAC is sensitivity with the total number of compressors. Also, the sensitivity analysis of the electricity price of this case is depicted in Fig. 7b. This figure illustrates that the electricity price is a modeling coefficient which has great impact on the TAC of the global optimum.

4.3. Example 3

The third case study is from Hallale and Liu (2001) including two hydrogen utility sources HP and CRU, six process units DHT, CNHT, JHT, NHT, IS4 and HCU, and one FGS. Here, CRU is an auxiliary

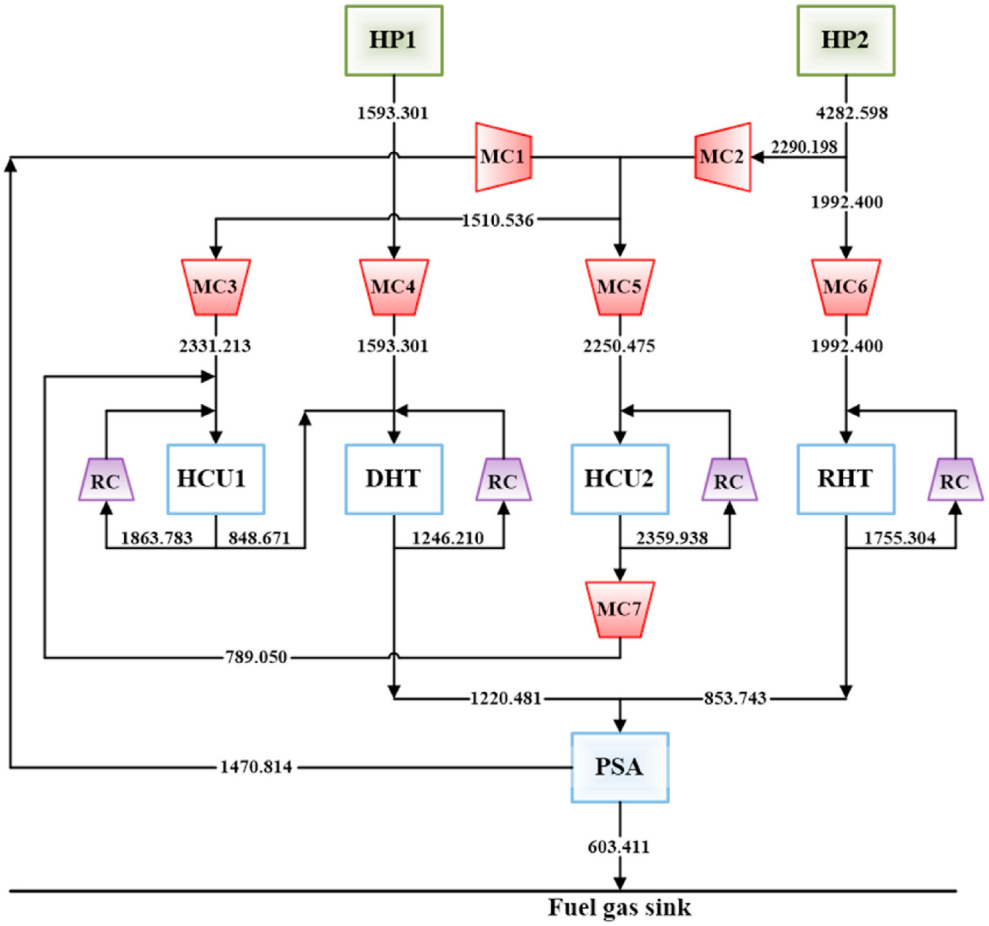

Fig. 12. The network design of the globally optimal solution for example 4.

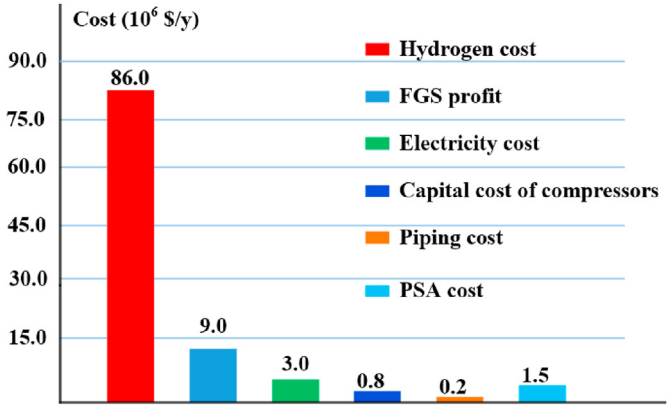

Fig. 13. Cost breakdown of the globally optimal solution for example 4.

source suppling fresh hydrogen gas with fixed flowrate and zero cost. Jagannath and Almansoori (2017) had researched this problem as a grass-roots synthesis example to minimize the total compression expense under the minimum fresh hydrogen supply (3387.766 kmol/h), regardless of other cost terms. Hence, in this case the flowrate of fresh hydrogen gas is fixed as 3387.766 kmol/h, ignoring hydrogen and piping expenses in TAC. The optimal network of Jagannath and Almansoori (2017) is shown in Fig. 10 with a TAC of 2,482,092.5 $/y. In the figure, there exist four makeup compressors and three recycle compressors respectively installed to lift the pressure of fresh hydrogen gases and the off-gases out of process units.

The proposed superstructure-based MINLM of this case includes 692 constraints, 452 continuous variables and 148 binary variables. After solving in 1198.6 s, the MINLM converges to the globally optimal solution and the network design is depicted in Fig. 11 with a TAC of 2,378,734.8 $/y. The cost breakdowns of the solutions obtained in literature and this work are listed in Table 3. Both solutions feature the same number of compressors. However, the compression power is reduced from 7742.9 to 7321.8 kW. The electricity expense is therefore decreased while the capital expense of compressors is increased slightly. As a consequence, the TAC is decreased by 4.2% (2,482,092.5 vs. 2,378,734.8 $/y). More importantly, the computing time is largely saved and the global optimality of the solution can be guaranteed. The sensitivity analysis of the total number of compressors (*NC*) for this case is depicted in Fig. 6c. It depicts that the TAC decreases from $NC = 4$ to 7 and increases from $NC = 7$ to 11. This figure clearly shows that the TAC of the global solution is sensitive with the total number of compressors. Moreover, the sensitivity analysis of the electricity price for this example is performed and presented in Fig. 7c. This figure demonstrates that the modeling coefficient (electricity price) has great impact on the TAC of the global optimum.

4.4. Example 4

The forth case study is a retrofit problem taken from Jagannath et al. (2018) which is modified as a grass-roots synthesis example in this research. It includes two hydrogen utility sources HP1 and HP2,

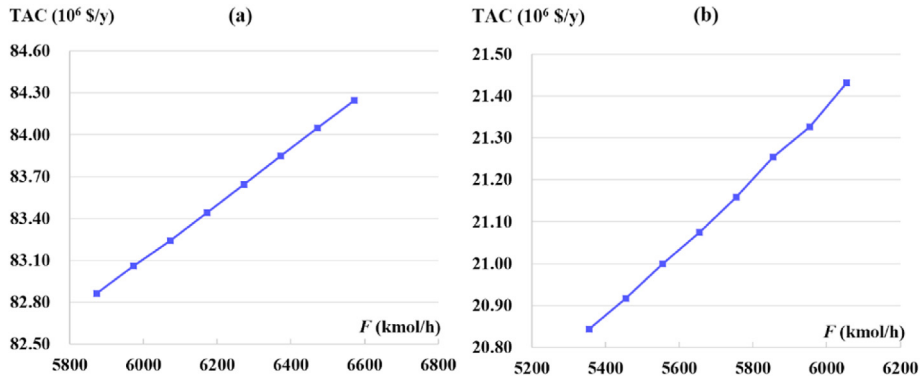

Fig. 14. The sensitivity analysis of fresh hydrogen flowrate (*F*): (a) example 4; (b) example 5.

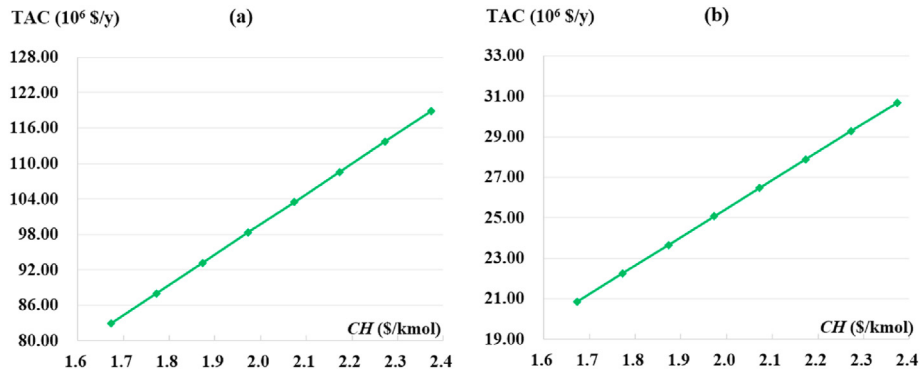

Fig. 15. The sensitivity analysis of fresh hydrogen price (*CH*): (a) example 4; (b) example 5.

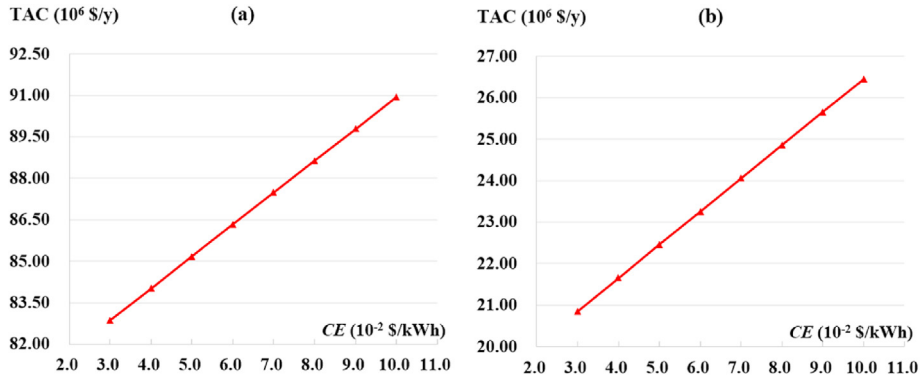

Fig. 16. The sensitivity analysis of electricity price (*CE*): (a) example 4; (b) example 5.

four process units HCU1, DHT, HCU2 and RHT, one PSA and one FGS. In this case, the objective function is to optimize the TAC which includes hydrogen utility cost, FGS profit, electricity cost and the capital costs of compressors, pipelines and PSA unit. The proposed superstructure-based MINLM has 439 constraints, 291 continuous variables and 95 binary variables. After running in 672.8 s, the MINLM converges to the globally optimal solution and its network design is presented in Fig. 12 with a TAC of 82,854,723.8 $/y. Fig. 12 depicts that eleven compressors are demanded to lift the pressures of the gas streams between hydrogen sources and sinks. Seven of them are makeup compressors while the other four are recycle compressors. All the cost-related terms (breakdowns) are respectively shown in Fig. 13. It illustrates that the hydrogen cost is the highest expense while other cost terms, such as the capital expenses of pipelines and PSA units, are relatively low. The sensitivity analysis of fresh hydrogen flowrate (*F*) for this case study is presented in Fig. 14a. It indicates the TAC increases monotonically along with fresh hydrogen demand. Therefore, it is reasonable to optimize the total compression expenses under the minimum fresh hydrogen flowrate, as studied in examples 1–3. In addition, the sensitivity analysis of fresh hydrogen price and electricity price for this case study are performed and depicted in Figs. 15a and 16a respectively. Such two figures both show that modeling coefficients have great impacts on the TAC of the global optimum.

4.5. Example 5

The last example is a real industrial case adopted from a refinery that is located at southern China. It includes three hydrogen utility sources namely HP, SRU and CRU, six process units namely RHT, HC,

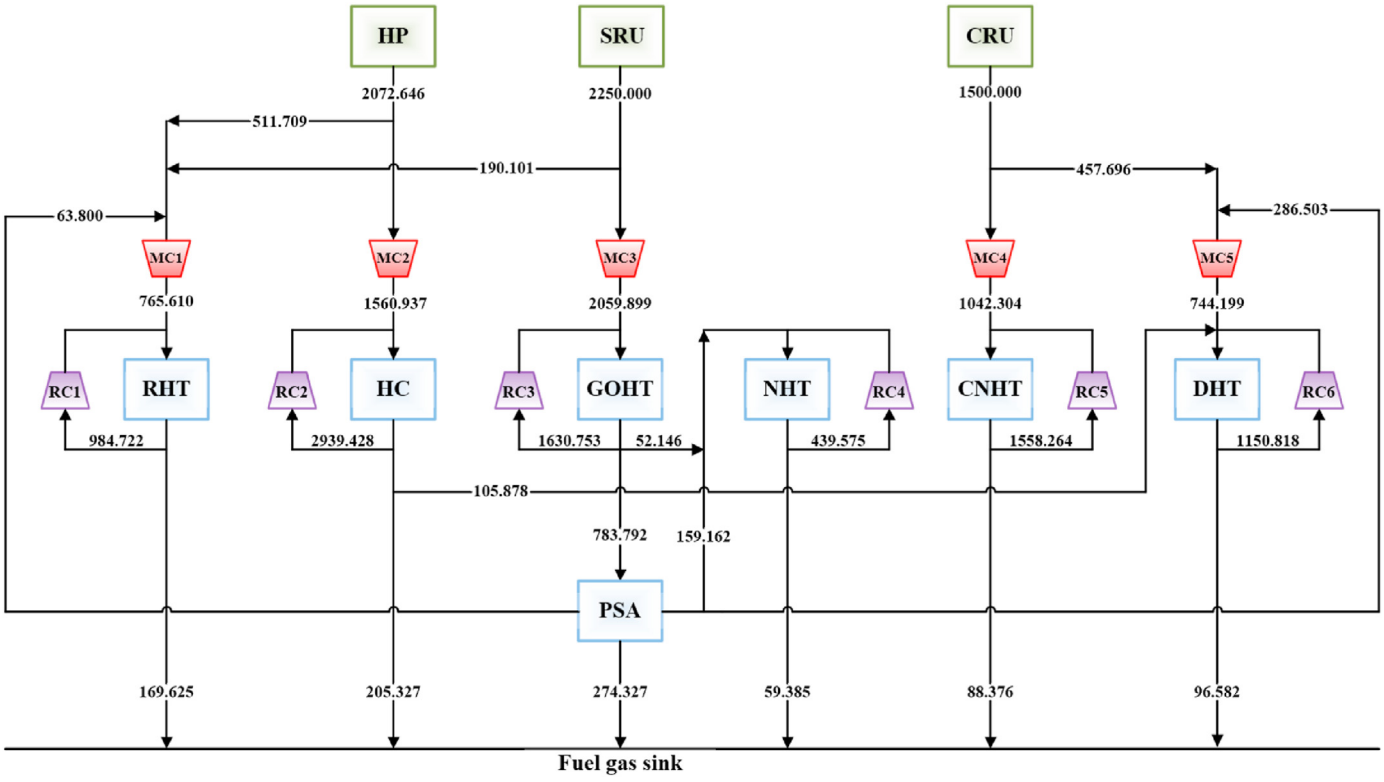

Fig. 17. The original network of example 5.

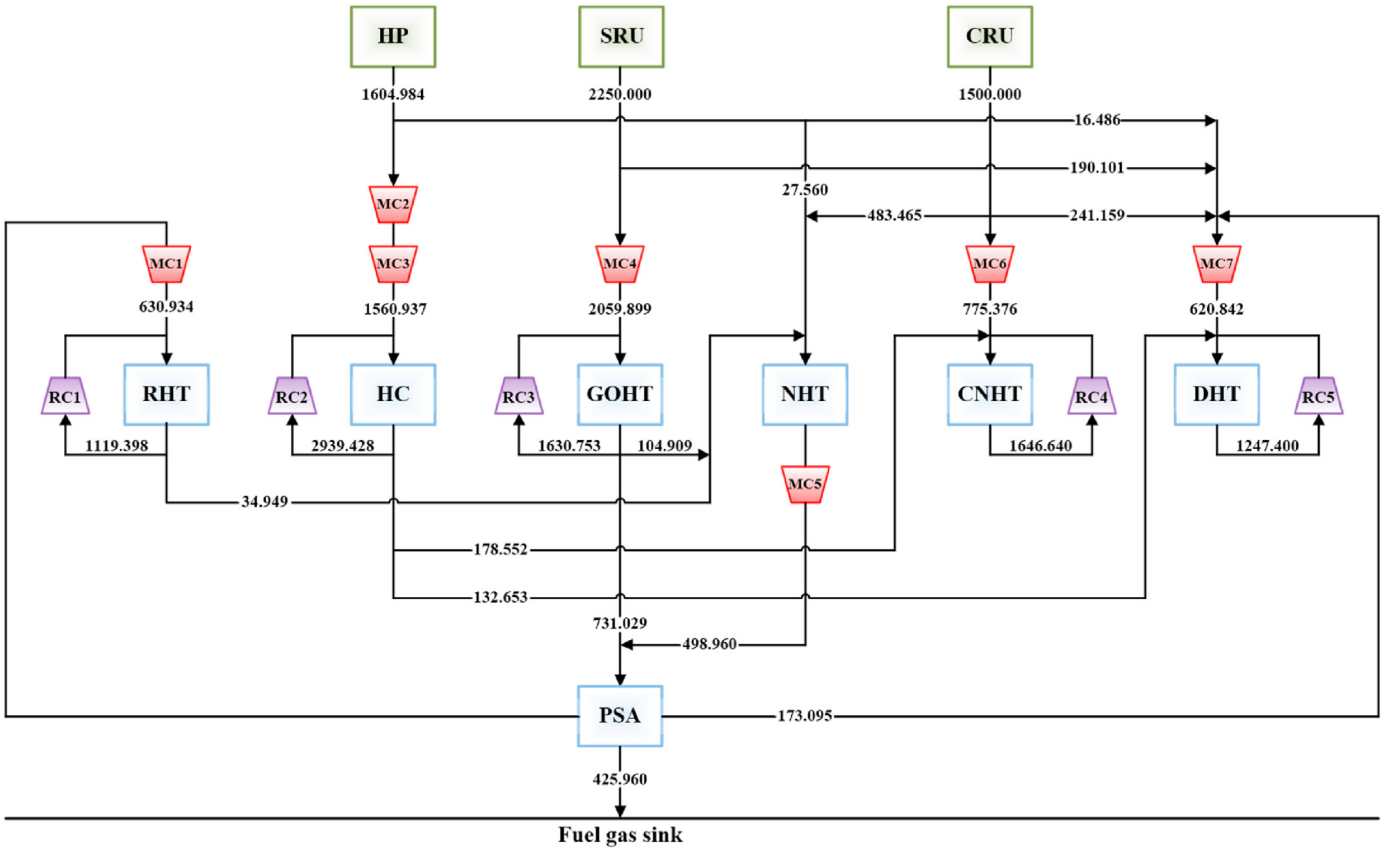

Fig. 18. The network design of the globally optimal solution for example 5.

Table 4
Solution comparison for example 5.

Item	Original solution	Solution in this work
Hydrogen flowrate (kmol/h)	5822.646	5354.984
Number of compressors	11	12
Compression power (kW)	9454.6	9283.4
Hydrogen cost ($/y)	30,376,063.3	23,522,151.7
FGS profit ($/y)	10,152,411.6	6,762,416.3
Electricity cost ($/y)	2,484,658.3	2,439,667.7
Capital cost of compressors ($/y)	682,723.9	674,969.6
PSA cost ($/y)	546,655.9	857,856.0
Piping cost ($/y)	119,531.6	110,956.5
TAC ($/y)	24,057,221.4	20,843,185.3

GOHT, NHT, CNHT and DHT, one PSA and one FGS. The utility sources SRU and CRU provide auxiliary fresh hydrogen gas with fixed flowrates and zero cost. The objective function is to minimize TAC, including hydrogen utility expense, FGS profit, electricity expense and the capital investment of compressor, pipeline and PSA unit. The original network design is shown in Fig. 17 with a TAC of 24,057,221.4 $/y. This figure shows the flowrate of fresh hydrogen supply is 5822.646 kmol/h and the total number of the demanded compressors is eleven, five being makeup ones and six being recycle ones respectively. The off-gas from process unit GOHT is routed to PSA for hydrogen purification. The off-gases of other process units including RHT, HC, NHT, CNHT and DHT are directly sent to FGS.

The proposed superstructure-based model for the case includes 651 constraints, 462 continuous variables and 192 binary variables. It is solved to global optimality in 2136.2 s and the TAC of the globally optimum is 20,843,185.3 $/y. The corresponding network design is depicted in Fig. 18. This figure depicts the flowrate of fresh hydrogen gas supplied to the network is 5354.984 kmol/h. Seven makeup compressors and five recycle compressors are needed to lift the pressures of the gas streams among hydrogen sources and sinks. The off-gases of process units GOHT and NHT are routed to PSA unit for hydrogen purification. The PSA unit sends its product gas to process units RHT and DHT. Only the residual gases of PSA unit are sent to FGS. Note that the inlet pressure of process unit HC is relatively high (13,789.5 kPa) and thus two makeup compressors (MC2 and MC3) are installed in series to reduce the compression ratio and power.

Table 4 lists the cost-related terms of the original solution and the globally optimal one. It shows that the TAC is reduced by 13.4% from 24,057,221.4 to 20,843,185.3 $/y. This outcome is mainly attributed to 8% reduction in fresh hydrogen supply (5822.646 vs. 5354.984 kmol/h). The cost of fresh hydrogen is thereby saved while the FGS profit is reduced. One more compressor is demanded (11 vs. 12) while the compression power is saved (9454.6 vs. 9283.4 kW), and hence both the capital and electricity expenses of compressors are saved. The sensitivity analysis of fresh hydrogen flowrate (F) is shown in Fig. 14b. It shows TAC is almost linearly related to hydrogen flowrate F and increases monotonically. Obviously, the TAC of the global optimum is sensitive with the flowrate of fresh hydrogen. In fact, the solution results highly depend on the input parameters of different modeling coefficients, including fresh hydrogen price, electricity price and so forth. To analyze the impacts of the input parameters, the hydrogen price (CH) and electricity price (CE) are varied for illustration purposes. The resultant TACs of the globally optimal solutions using different CH and CE are respectively presented in Figs. 15b and 16b. Such two figures clearly illustrate TAC increases monotonically along with the increase of hydrogen and electricity prices. Therefore, the input parameters of modeling coefficients have considerable impact on the optimization and solution results. All the above demonstrate the capabilities of the proposed model.

5. Conclusions

This work presents a new superstructure for the grass-roots synthesis of hydrogen networks. The corresponding mathematical model can balance the richness of structure possibilities and the computational difficulty. This is achieved by assigning compressor at different positions: after the outlet splitter of hydrogen sources or after a set of mixer-splitter nodes. In this way, both the dedicated compressors and shared compressors can exist in the proposed superstructure while the pressures of these compressors are known beforehand. Based on this, a new MINLM is modelled for hydrogen networks synthesis in which the constraint of compression power is written as linear equation, and thus the nonlinearities of the MINLM only arise from bilinear and concave terms. Four literature examples and one industrial case are globally solved within 40 min to illustrate the applicability of the superstructure-based MINLM. The solution results of examples 1–3 indicate the TACs and computing time are decreased significantly. Examples 4 and 5 shows the MINLM can be applied to hydrogen networks synthesis integrating PSA as purification unit. The sensitive analysis in each example indicates that the input data of modeling coefficients have great impacts on the global optimum.

The sensitive analysis in example 4 and 5 illustrates the solution result is sensitive with the flowrate of fresh hydrogen supply. Thus, it is meaningful to consider hydrogen demand fluctuations and dynamic flows for hydrogen networks synthesis which will be studied in further. Another further work is to apply the proposed superstructure-based model to the retrofit design of hydrogen networks. The mathematical model of retrofit design problem is considerably different from that of the grass-roots synthesis problems, due to the existence of the devices which are already present.

CRediT authorship contribution statement

Chenglin Chang: Methodology, Conceptualization, Writing - original draftWriting – original draft, preparation. **Zuwei Liao:** Supervision. **Miguel J. Bagajewicz:** Writing - review & editing-Writing – review & editing, Superstructure and Reviewing.

Declaration of competing interest

The authors declare that they have no known competing financial interests or personal relationships that could have appeared to influence the work reported in this paper.

Acknowledgements

The financial supports of this research are funded by the Project of National Natural Science Foundation of China (No. 22008210 & 21822809 & 21978256), China Postdoctoral Science Foundation (No. 2019TQ0275 & 2020M671723), the Foundation of State Key Laboratory of High-efficiency Utilization of Coal and Green Chemical Engineering (Grant No. 2018-K23). Miguel J. Bagajewicz appreciates Rio de Janeiro State University for its scholarship of Visiting Researcher - PAPD Program.

Appendix A. Supplementary data

Supplementary data to this article can be found online at https://doi.org/10.1016/j.jclepro.2021.126022.

References

Alves, J.J., Towler, G.P., 2002. Analysis of refinery hydrogen distribution systems. Ind. Eng. Chem. Res. 41 (23), 5759e5769.

Bandyopadhyay, R., Alkilde, O.F., Upadhyayula, S., 2019. Applying pinch and exergy analysis for energy efficient design of diesel hydrotreating unit. J. Clean. Prod. 232, 337–349.

Brooke, A., Kendrick, D., Meeraus, A., Raman, R., 2005. GAMS: A Users Guide. GAMS Development, Washington, DC.

Chang, C., Peccini, A., Wang, Y., Costa, A.L.H., Bagajewicz, M.J., 2020. Globally optimal synthesis of heat exchanger networks. Part I: minimal networks. AIChE J. 66 (7), e16267.

Čuček, L., Boldyryev, S., Klemeš, J.J., Kravanja, Z., Krajačić, G., Varbanov, P.S., Duić, N., 2019. Approaches for retrofitting heat exchanger networks within processes and Total Sites. J. Clean. Prod. 211, 884–894.

Deng, C., Liu, J., Zhou, Y., Feng, X., 2019. Design of hydrogen network integrated with the shared purifier in hydrogen production plant. Ind. Eng. Chem. Res. 58 (24), 10466–10481.

Deng, C., Zhu, M., Liu, J., Feng, X., 2020. Systematic retrofit method for refinery hydrogen network with light hydrocarbons recovery. Int. J. Hydrogen Energy 45 (38), 19391–19404.

Ebrahimi, A., Ghorbani, B., Ziabasharhagh, M., 2020. Pinch and sensitivity analyses of hydrogen liquefaction process in a hybridized system of biomass gasification plant, and cryogenic air separation cycle. J. Clean. Prod. 258, 120548.

Elkamel, A., Alhajri, I., Almansoori, A., Saif, Y., 2011. Integration of hydrogen management in refinery planning with rigorous process models and product quality specifications. Int. J. Process Syst. Eng. 1 (3), 302–330.

Elsherif, M., Manan, Z.A., Kamsah, M.Z., 2015. State-of-the-art of hydrogen management in refinery and industrial process plants. J. Nat. Gas Sci. Eng. 24, 346–356.

Faria, D.C., Bagajewicz, M.J., 2012. A new approach for global optimization of a class of MINLP problems with applications to water management and pooling problems. AIChE J. 58 (8), 2320–2335.

Fonseca, A., Sá, V., Bento, H., Tavares, M.L.C., Pinto, G., Gomes, L.A.C.N., 2008. Hydrogen distribution network optimization: a refinery case study. J. Clean. Prod. 16 (16), 1755–1763.

Hallale, N., Liu, F., 2001. Refinery hydrogen management for clean fuels production. Adv. Environ. Res. 6 (1), 81–98.

Hong, X., Liao, Z., Sun, J., Jiang, B., Wang, J., Yang, Y., 2019. Transshipment type heat exchanger network model for intra- and inter-plant heat integration using process streams. Energy 178, 853–866.

Huang, L., Liu, G., 2019. Optimization of the hydrogen separator based on the hydrogen network integration. J. Clean. Prod. 235, 1399–1408.

Jagannath, A., Almansoori, A., 2017. A mathematical model for optimal compression costs in the hydrogen networks for the petroleum refineries. AIChE J. 63 (9), 3925–3943.

Jagannath, A., Elkamel, A., Karimi, I.A., 2014. Improved synthesis of hydrogen networks for refineries. Ind. Eng. Chem. Res. 53 (44), 16948–16963.

Jagannath, A., Madhuranthakam, C.M.R., Elkamel, A., Karimi, I.A., Almansoori, A., 2018. Retrofit design of hydrogen network in refineries: mathematical model and global optimization. Ind. Eng. Chem. Res. 57 (14), 4996–5023.

Jhaveri, N., Mohanty, B., Khanam, S., 2014. Mathematical modeling and optimization of hydrogen distribution network used in refinery. Int. J. Hydrogen Energy 39 (1), 339–348.

Kang, L., Jiang, Y., Liu, Y., 2019. Impacts of synthesis schemes on economy and flexibility of hydrogen networks. Chem. Eng. Sci. 207, 1159–1174.

Khajehpour, M., Farhadi, F., Pishvaie, M.R., 2009. Reduced superstructure solution of MINLP problem in refinery hydrogen management. Int. J. Hydrogen Energy 34 (22), 9233–9238.

Kumar, A., Gautami, G., Khanam, S., 2010. Hydrogen distribution in the refinery using mathematical modeling. Energy 35 (9), 3763–3772.

Li, H., Liao, Z., Sun, J., Jiang, B., Wang, J., Yang, Y., 2019. Modelling and simulation of two-bed PSA process for separating H2 from methane steam reforming. Chin. J. Chem. Eng. 27 (8), 1870–1878.

Li, H., Liao, Z., Sun, J., Jiang, B., Wang, J., Yang, Y., 2020. Simultaneous design of hydrogen allocation networks and PSA inside refineries. Ind. Eng. Chem. Res. 59 (10), 4712–4720.

Liao, Z., Wang, J., Yang, Y., Rong, G., 2010. Integrating purifiers in refinery hydrogen networks: a retrofit case study. J. Clean. Prod. 18 (3), 233–241.

Liu, X., Liu, J., Deng, C., Lee, J., Feng, X., 2020. Synthesis of refinery hydrogen network integrated with hydrogen turbines for power recovery. Energy 201, 117623.

Liu, F., Zhang, N., 2004. Strategy of purifier selection and integration in hydrogen networks. Chem. Eng. Res. Des. 82 (10), 1315–1330.

Lou, Y., Liao, Z., Sun, J., Jiang, B., Wang, J., Yang, Y., 2019. A novel two-step method to design inter-plant hydrogen network. Int. J. Hydrogen Energy 44 (12), 5686–5695.

Marques, J.P., Matos, H.A., Oliveira, N.M.C., Nunes, C.P., 2017. State-of-the-art review of targeting and design methodologies for hydrogen network synthesis. Int. J. Hydrogen Energy 42 (1), 376–404.

Rezaie, F., Roshandel, R., Hamidi, A.A., 2020. Hydrogen management in refineries: retrofitting of hydrogen networks, electricity and ammonia production. Chemical Engineering and Processing-Process Intensification 157, 108118.

Sardashti Birjandi, M.R., Shahraki, F., Birjandi, M.S., Nobandegani, M.S., 2014. Application of global optimization strategies to refinery hydrogen network. Int. J. Hydrogen Energy 39 (27), 14503–14511.

Shehata, W.M., Shoaib, A.M., 2015. Simple optimization method for partitioning purification of hydrogen networks. Egyptian Journal of Petroleum 24 (1), 87–95.

Towler, G.P., Mann, R., Serriere, A.J.L., Gabaude, C.M.D., 1996. Refinery hydrogenManagement: cost analysis of chemically-integrated facilities. Ind. Eng. Chem. Res. 35 (7), 2378e2388.

Umana, B., Shoaib, A., Zhang, N., Smith, R., 2014. Integrating hydroprocessors in refinery hydrogen network optimisation. Appl. Energy 133, 169–182.

Wang, J., Lou, H.H., Yang, F., Cheng, F., 2016. Development and performance evaluation of a clean-burning stove. J. Clean. Prod. 134, 447–455.

Wei, L., Liao, Z., Jiang, B., Wang, J., Yang, Y., 2017. Automatic design of multi-impurity refinery hydrogen networks using mixing potential concept. Ind. Eng. Chem. Res. 56 (23), 6703–6710.

Wei, L., Shen, Y., Liao, Z., Sun, J., Jiang, B., Wang, J., Yang, Y., 2019. Balancing between risk and profit in refinery hydrogen networks: a Worst-Case Conditional Value-at-Risk approach. Chem. Eng. Res. Des. 146, 201–210.

Zhang, Q., Li, J., Feng, X., 2020. Thermodynamic principle based hydrogen network synthesis with hydrorefining feed oil sulfur content variation for total exergy minimization. J. Clean. Prod. 256, 120230.